

The impact of the representation of soil-vegetation-atmosphere interaction upon snow processes

E. A. KOWALCZYK & J. L. MCGREGOR

CSIRO Atmospheric Research, Private Bag No. 1, Aspendale, Victoria 3195, Australia

e-mail: eva.kowalczyk@dar.csiro.au

Abstract Two soil-vegetation-atmosphere transfer (SVAT) schemes, with different degrees of complexity, were incorporated into the CSIRO Division of Atmospheric Research Limited Area Model (DARLAM). Both schemes were used to compute the spatial and temporal evolution of fluxes of momentum, energy and water, as well as snow accumulation, ablation, runoff, and soil freezing in a region of high latitude. Both schemes use the same treatment for soil subsurface thermal and hydrological processes, as well as for snow. In the first SVAT scheme, a "big-leaf" approach is used to represent vegetation. Each computational grid box is partitioned into a vegetation part and a bare ground part; the model computes the fluxes for each fraction separately, with no aerodynamic or radiative interaction between the vegetation and the ground. In the second scheme, the vegetation is spread across the grid and placed above the ground, allowing for full interaction; a combined energy balance is calculated for the whole system. The soil model solves Richards' equation for moisture transport over six soil layers. Similarly, a six-layer model is used to compute heat conduction. A parameterization of a soil freeze/thaw cycle is also included in the model. The snow model computes the temperature, snow density and thickness of three snowpack layers. The experiment consists of two 2-year integrations, forced at the lateral boundaries by NCEP reanalyses. The results are presented for soil-vegetation-atmosphere interaction, in regards to the calculation of snow processes and surface fluxes.

Key words snow processes; vegetation processes; vegetation parameters; SVAT schemes; atmospheric model; limited area model; computer simulation; snow-atmosphere exchange

INTRODUCTION

In high latitudes, where snow and soil ice constitute an important part of the environment, the interactions between vegetation and snow strongly affect mass and energy exchanges. Snow has the highest solar reflectivity of all natural surfaces, reducing strongly the available energy at the surface. The presence of vegetation has a masking effect, reducing the overall surface albedo; however, in the case of a dense canopy, the snow is sheltered from the incoming solar radiation. The hydrological cycle is affected by seasonal freezing and thawing of the ground, which again is affected by snow depth and snow melting.

This paper examines the impact on snow and soil processes of employing, within one host atmospheric model, two SVAT schemes of different complexity. The experiment described consists of a 2-year integration, covering the period from June 1996 to June 1998.

MODEL DESCRIPTION

The host model—the CSIRO Division of Atmospheric Research Limited Area Model (DARLAM)—is a two-time-level semi-implicit hydrostatic primitive equations model, originally described by McGregor (1987). Semi-Lagrangian advection is performed in the horizontal. The departure points required for each time step are determined by the scheme of McGregor (1993). The requisite updating of variables is carried out with bicubic Lagrange interpolation. Vertical advection is carried out as a split process using the Van Leer (1974) total-variation diminishing scheme. Long-wave radiative contributions are provided by a recent version of the Fels & Schwarzkopf (1975) scheme and the short-wave scheme is an updated version of the Lacis & Hansen (1974) scheme, with radiative clouds diagnosed from relative humidity. The cumulus convection scheme is an Arakawa (1972) mass flux scheme as modified extensively by H. B. Gordon (CSIRO, personal communication, 1993). A more complete description of these parameterizations is given by McGregor *et al.* (1993).

The DARLAM model was primarily developed for regional climate modelling, but for some years it has been run automatically twice a day as a CSIRO in-house forecasting system.

Description of SVAT1 and SVAT2 schemes

In the SVAT1 scheme, a commonly employed “big-leaf” approach is used to represent vegetation. Each computational grid box is partitioned into a vegetation part, σ_f , and a bare ground part $(1 - \sigma_f)$; the model computes the fluxes for each fraction separately, with no aerodynamic or radiative interaction between the vegetation and the ground. Weighted averages are used to describe temperature and fluxes for a whole grid element, (as illustrated for sensible heat flux in Fig. 1). The fluxes are parameterized following Monin-Obukhov similarity theory (for details, see Kowalczyk *et al.*, 1991). The total water vapour flux over an area is assumed to arise from evaporation from the

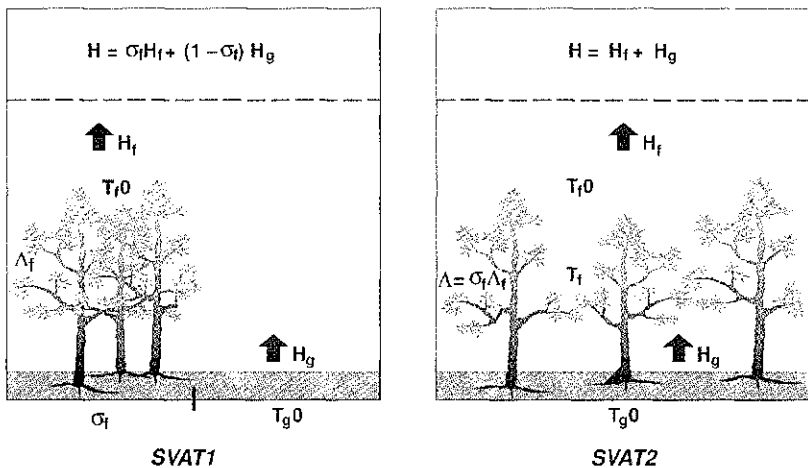


Fig. 1 Vegetation representation in SVAT1 and SVAT2.

ground, E_g , and evaporation from the canopy, E_f . The latter comprises evaporation from the fraction of canopy covered with water, and transpiration from the remaining part of the dry canopy, E_{tr} . A separate mass balance equation for the canopy-intercepted rain is carried out. Transpiration is parameterized using bulk stomatal resistance, r_s , which depends on a range of factors including atmospheric conditions, availability of soil moisture, and vegetation type. The formulation is based on Noilhan & Planton (1989). The parameters required for the vegetation description in SVAT1 are: unconstrained stomatal resistance, r_s^{min} , fraction of vegetation, σ_f , leaf area index, Λ_f , roughness length, z_{0f} , albedo of foliage, α_f and emissivity of foliage, ϵ_f .

In the SVAT2 scheme, the vegetation is spread across the grid with leaf area index $\Lambda = \sigma_f \Lambda_f$ (note that Λ_f is the same for both schemes). The vertical placement of the canopy above the ground allows for full aerodynamic and radiative interaction between vegetation and the ground. The total grid flux is the sum of the flux from the soil to the canopy air space and the canopy to the atmosphere (see Fig. 1).

Similarly to SVAT1, the latent heat from vegetation includes transpiration and evaporation of the intercepted rainfall. However, the stomatal resistance, r_s , is calculated in a more complex manner, as described by Wang & Leuning (1998).

For radiative exchange purposes the canopy is treated as a screen with transmission, τ , derived in a complex way as described by Wang & Leuning (1998). At the soil level, the incoming solar radiation is given by $\tau R_s \downarrow$, where $R_s \downarrow$ is the incoming short-wave radiation. The incoming long-wave radiation has two components: the incoming long-wave sky irradiance $R_L \downarrow$ and the downward radiation from foliage, i.e.:

$$R_L^g \downarrow = \tau R_L \downarrow + (1 - \tau) \epsilon_f \sigma T_f^4 \quad (1)$$

where σ is the Stefan-Boltzmann constant and T_f is vegetation temperature. For the foliage layer, the incoming long-wave radiation is:

$$R_L^f \downarrow = (1 - \tau) R_L \downarrow + (1 - \tau) \epsilon_g \sigma T_{g0}^4 \quad (2)$$

where ϵ_g is the emissivity of the ground and T_{g0} is ground temperature.

Extra parameters required for the vegetation description include leaf angle distribution, typical leaf dimension, leaf shelter factor and vegetation height. The height and leaf area index are used for the calculation of turbulent resistances for transfer from soil to canopy and canopy to reference level. The canopy roughness length in SVAT2 is a function of leaf area index and canopy height (Raupach *et al.*, 1997), while in SVAT1 the canopy roughness is prescribed from the data set of Dorman & Sellers (1989). In both schemes a similar treatment is used to reduce the vegetation cover for increased snow depth. The snow-free bare ground roughness length, z_0 in SVAT1 is 0.01 m, decreasing with snow depth. In SVAT2, z_0 is usually smaller than in SVAT1, as it applies to transfer from ground level to canopy air space rather than the reference level.

Soil treatment

The treatment of soil thermal and hydrological processes is the same in both schemes. The soil model solves Richards' equations for soil moisture content, η :

$$\frac{\partial \eta}{\partial t} = -\frac{\partial}{\partial z} \left(K - K \frac{\partial \psi}{\partial z} \right) + r_i(z) \quad (3)$$

The relationships between the hydraulic conductivity, K , the matrix potential, ψ and the soil moisture content follow Clapp & Hornberger (1978). The r_i terms include snowmelt, runoff, drainage and root extraction for evapotranspiration. The top boundary condition of equation (3) is given by the infiltration rate, which depends on rainfall, snowmelt, evaporation, surface runoff and soil hydrological properties. At the bottom, gravitational drainage occurs to restore the water profile to the field capacity. Similarly, a six-layer model is used for conduction of heat; as a top boundary condition, the net heat flux at the surface is applied. A parameterization of a soil freeze/thaw cycle is also included.

Snow model

The snow albedo calculations are based on Dickinson *et al.* (1993), with the basic dependence of albedo on solar zenith angle, snow depth and snow density included. The change in the total snow mass is based on a mass budget equation that includes the snowfall and rainfall rates, the rate of sublimation, and snowmelt. Rain falling on snow freezes at the surface, releasing latent heat. The discretization of the snowpack depth into layers changes with snowfall and snowmelt, sublimation and densification. When the layer thickness changes, the mass and heat content of the layers is redistributed accordingly. In the model, the changes in snow density are parameterized using empirical relationships from Anderson (1976). The snow density increases with time due to compaction and settling processes, affecting the temperature of the snow through changes to the snow thermal conductivity. Snow density is also used for the snow albedo calculations. At the bottom of the snowpack boundary, the energy balance is influenced by the ground heat flux through the soil surface. At the top, the energy balance of the snow cover is influenced by the surface net heat flux.

In the model, the snow cover interacts with vegetation in the following ways: firstly, it reduces the fractional vegetation cover due to vegetation being partially buried under the snow; secondly, the overall surface albedo is decreased in the presence of vegetation; and thirdly, snow under the canopy is sheltered from solar radiation while receiving long-wave radiation emitted from the vegetation.

SIMULATION RESULTS

For the experiment, DARLAM has a horizontal resolution of 40 km with a domain as shown in Fig. 2. The time step is 10 min. The atmospheric variables are forced at the lateral boundaries by 6-hourly NCEP reanalyses. At the beginning of the simulation (June 1995), the soil temperatures are initialized to the observed air temperatures and soil moisture to half the field capacity. Vegetation classification and distribution is as described by Dorman & Sellers (1989) (which include needleleaf-evergreen and needleleaf-deciduous trees, and tundra), while soil types follow the classification of Zobler (1988).

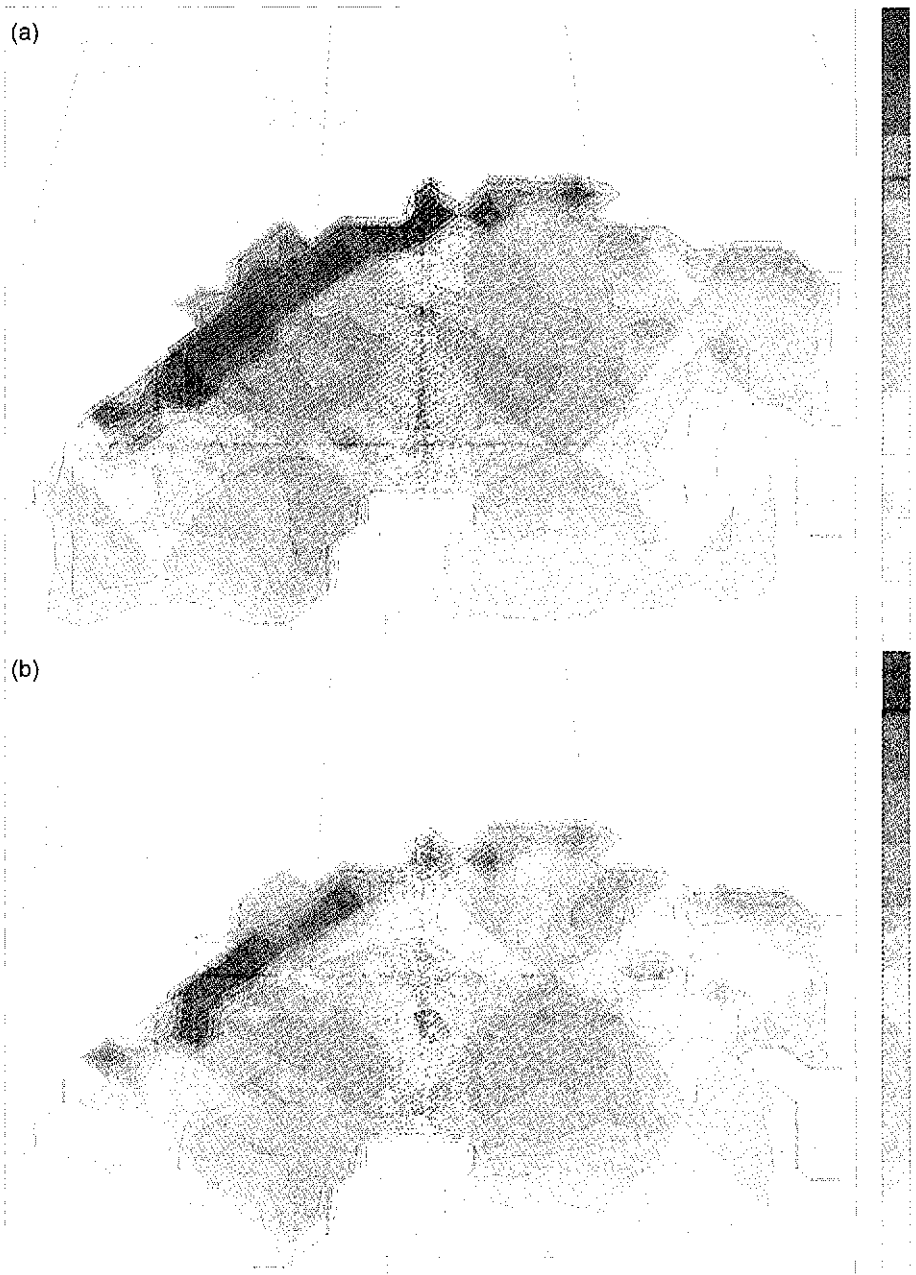


Fig. 2 Mean snow depth distribution for winter (DJF) produced by (a) SVAT1, and (b) SVAT2.

Two regions covering northern Sweden and Norway were selected for comparison with the compiled climatology of observed data reported by Christensen *et al.* (1998). The first region covers northern Sweden with the exclusion of the high mountains, while the second region covers the mountain area. Table 1 presents the seasonal means

Table 1 Summary of observed (as reported by Christenson *et al.*, 1998) and model-derived seasonal statistics for northern Sweden (a) with the exclusion of the mountains, and (b) for the mountain area.

	P_w (mm day ⁻¹)	R_w (mm day ⁻¹)	S_w (cm)	P_s (mm day ⁻¹)	R_s (mm day ⁻¹)	S_s (cm)
(a) <i>Excluding the mountains:</i>						
Obs.	1.2	<0.3	17	1.0	1.8	15
Obs. SMHI			>40			>50
SVAT1	1.0	0.2	47	0.7	1.2	52
SVAT2	0.9	0.5	25	0.7	0.9	15
(b) <i>Mountain area:</i>						
Obs.	2.1	0.5	14	1.4	2.2	12
Obs. SMHI			>70			>80
SVAT1	1.2	0.1	67	0.7	1.4	88
SVAT2	1.3	0.4	35	0.8	1.2	37

P_w, P_s : mean precipitation, R_w, R_s : runoff, and S_w, S_s : snow depth, in winter (DJF) and spring (MAM), respectively.

Snow depth observations from SMHI reports are also included.

for rainfall, runoff and snow depth as computed by both schemes, and as reported by Christensen *et al.* (1998).

In the first area (Table 1(a)), the precipitation rate is slightly underestimated in comparison with the observed values in both seasons. For the mountain region (Table 1(b)) the larger underestimation of the precipitation may be related to the simulation spatial resolution. The resolution of 40 km does not appear to be adequate to resolve the high topography terrain.

There are significantly greater simulated snow depths than the values reported in Christensen *et al.* (1998). Their snow data were derived from Foster & Davy (1988), based on low-altitude measurements; hence they may underestimate the actual snow depth. Qualitative comparison with the Swedish Meteorological and Hydrological Institute (SMHI) (1996, 1997, 1998) snow depth observations for northern Sweden indicates that the winter snow depth for the two simulated seasons was in excess of 40 cm, while in spring it was in excess of 50 cm; hence the SVAT1 simulation appears to be closer to these observations. The simulated snow depth in the mountains is higher than in the first region, and this agrees with the observation of snow depth as reported by SMHI. Both schemes were able to reasonably simulate snow cover distribution. Figure 2 shows the winter mean snow cover as produced by SVAT1 and SVAT2. Detailed analysis of the snow cover evolution indicates that the cooler surface in SVAT1 allowed increased snow deposition, hence increased surface albedo, and decreased roughness length.

Table 2 Simulated mean fluxes and surface albedo for winter (DJF) for SVAT1 and SVAT2.

	R_{net} (W m ⁻²)	H (W m ⁻²)	LE (W m ⁻²)	α_s
SVAT1	-39	-31	0	0.66
SVAT2	-35	-35	5	0.55

R_{net} : net radiation; H : sensible heat flux; LE : latent heat flux; α_s : surface albedo.

In SVAT2, the winter radiative cooling of the ground was reduced by more vigorous heat exchange between the warm air advected from the ocean and the underlying cool surface. (On the other hand, for the summer months in SVAT2, more vigorous heat exchange between the cool air advected from the ocean and the underlying warm surface, produced lower surface temperatures, which were closer to the observations than for SVAT1.) The formulation of the aerodynamic exchange between soil, vegetation and the atmosphere, including the interaction between the soil and the vegetation, produced larger magnitude (negative) sensible heat fluxes. Table 2 presents the mean net radiation fluxes, sensible and latent heat fluxes for both schemes for the winter season. Net radiation in winter is lower in SVAT1 due to higher surface albedo, while latent heat flux is lower due to the cooler surface. Additional radiative heating of the ground surface in SVAT2 came from the second term in equation (1). It is possible that the vegetation distribution and type (mainly trees), as derived from Dorman & Sellers (1989), are not adequately represented in the 40-km grid, leaving small shrubs and grasses greatly unrepresented. With trees replaced by shrubs and grasses, the smaller roughness length will produce less exchange and thus lower surface temperatures. (In SVAT2 the vegetation height and leaf area index are used for the calculation of aerodynamic resistances.)

The simulated runoff is underestimated in both schemes in spring (Table 1) due to lower precipitation rates in the model. The mean winter runoff is higher in the SVAT2 simulation due to the warmer surface; however in spring, SVAT1 produced more runoff due to higher snowmelt. The melting of the snow in the mountains occurred in

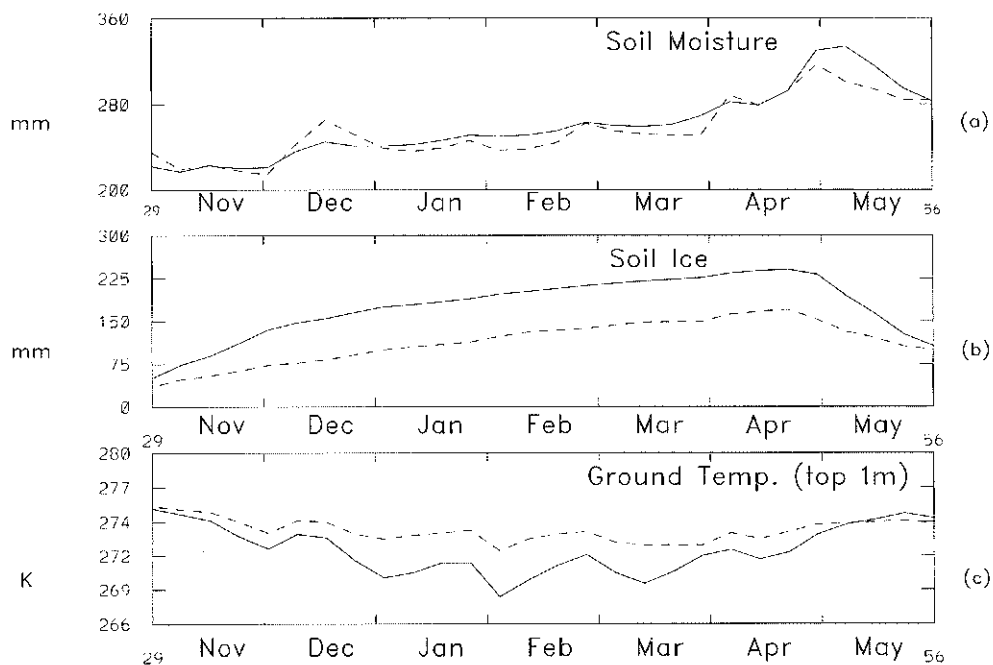


Fig. 3 Time evolution of soil moisture, frozen soil moisture and ground temperature (the top 1 m) for the period November 1997–May 1998. (Solid line: SVAT1; dashed line: SVAT2.)

the SVAT2 run until the end of May, but in the SVAT1 run until the end of June (which was closer to the observations).

Greater cooling of the ground in SVAT1 than in SVAT2 produced increased frost penetration. Figure 3 shows the time evolution of soil moisture, frozen soil moisture and ground temperature (the top 1 m) for the period November 1997–May 1998. The mean temperature of the top 1 m of soil in SVAT1 was lower than in SVAT2 by up to 3 K. The moisture variation in SVAT2 is slightly larger due to more unfrozen soil pore space available for water diffusion (the soil ice becomes a part of the solid matrix, reducing the available pore space for transfer).

CONCLUSIONS

Both schemes captured reasonably well the snow cover distribution in the simulated domain. SVAT1 accumulated more snow and produced more soil ice due to lower surface temperatures, and was closer to the SMHI observations. The snow depth of SVAT2 was smaller due to a warmer surface produced by more vigorous heat exchange between the cool surface and warmer air advected from the ocean. Consequently, SVAT2 simulated snow melting earlier than observed. It appears that the present formulation of the surface exchange between soil, vegetation and atmosphere in SVAT2 requires finer spatial representation of vegetation types and distribution. Especially, parameters such as vegetation height and *LAI* should vary geographically rather than being assigned to just a particular vegetation type. It was found that the more elaborate SVAT2 scheme produced more accurate summer temperatures than the SVAT1 scheme.

REFERENCES

- Arakawa, A. (1972) Design of the UCLA general circulation model: numerical simulation of weather and climate. *Tech. Report no. 7, Dept. Meteorol., Univ. of California, Los Angeles, California, USA.*
- Anderson, E. A. (1976) A point energy and mass balance model of snow cover. *Office of Hydrology, NOAA Tech. Report NWS no. 19, Washington DC, USA.*
- Christensen, O. B., Christensen, J. H., Machenhauer, B. & Botzet, M. (1998) Very high-resolution regional climate simulations over Scandinavia - present climate. *J. Climate* **11**, 3204–3229.
- Clapp, R. B. & Hornberger, G. M. (1978) Empirical equations for some soil hydraulic properties. *Wat. Resour. Res.* **14**, 601–604.
- Dickinson, R. E., Henderson-Sellers, A. & Kennedy, P. J. (1993) Biosphere-Atmosphere Transfer Scheme (BATS) version 1c as coupled to the NCAR Community Climate Model. *NCAR Tech. note NCAR/TN-387+STR, National Center for Atmospheric Research, Boulder, Colorado, USA.*
- Dorman, J. L. & Sellers, P. J. (1989) A global climatology of albedo, roughness length and stomatal resistance for atmospheric general circulation models as represented by the simple biosphere model (SiB). *J. Appl. Met.* **28**, 833–855.
- Fels, S. B. & Schwarzkopf, M. D. (1975) The simplified exchange approximation: a new method for radiative transfer calculations. *J. Atmos. Sci.* **32**, 1475–1488.
- Foster, D. J. & Davy, D. R. (1988) Global snow depth climatology. *Publ. AFETAC/TN-88/006, US Air Force.*
- Kowalczyk, E. A., Garratt, J. R. & Krummel, P. B. (1991) A soil-canopy scheme for use in a numerical model of atmosphere—1D stand-alone model. *Res. Tech. Paper no. 23, CSIRO Atmos. Res., Aspendale, Victoria, Australia.*
- Lacis, A. A. & Hansen, J. E. (1974) A parameterization for the absorption of solar radiation in the earth's atmosphere. *J. Atmos. Sci.* **31**, 118–133.
- McGregor, J. L. (1987) Accuracy and initialization of a two-time-level split semi-Lagrangian model. In: *Short- and Medium-Range Numerical Weather Prediction* (ed. by T. Matsuno), 233–243. Special vol., Met. Soc. Japan, Tokyo.
- McGregor, J. L. (1993) Economical determination of departure points for semi-Lagrangian models. *Mon. Weath. Rev.* **121**, 221–230.

- McGregor, J. L., Gordon, H. B., Watterson, I. G., Dix, M. R. & Rotstayn, L. D. (1993) The CSIRO 9-level atmospheric general circulation model. *Res. Tech. Paper no. 26, CSIRO Atmos. Res., Aspendale, Victoria, Australia.*
- Noilhan, J. & Planton, S. (1989) A simple parameterization of land surface processes for meteorological models. *Mon. Weath. Rev.* **117**, 536–549.
- Raupach, M. R., Finkelde, K. & Zhang, L. (1997) Soil Canopy Atmosphere Model; description and comparison with field data. *Res. Tech. Paper no. 132, CSIRO Centre for Environmental Mechanics, Canberra, ACT, Australia.*
- SMHI (1996) *Vader och Vatten* (Weather and Water, in Swedish), vols 10–12 (ed. by C. E. Karlstrom). Swedish Meteorological and Hydrological Institute, Norrkoping, Sweden.
- SMHI (1997) *Vader och Vatten*, vols 1–12 (ed. by C. E. Karlstrom). SMHI, Norrkoping, Sweden.
- SMHI (1998) *Vader och Vatten*, vols 1–5 (ed. by C. E. Karlstrom). SMHI, Norrkoping, Sweden.
- Van Leer, B. (1974) I. Towards the ultimate conservative difference scheme. II. Monotonicity and conservation combined in a second-order scheme. *J. Comput. Phys.* **14**, 361–370.
- Wang, Y. P. & Leuning, R. (1998) A two-leaf model for canopy conductance, photosynthesis and partitioning of available energy. *Agric. For. Met.* **91**, 89–111.
- Zobler, L. (1988) A world soil file for global climate modeling. *NASA Tech. Memo. no. 87802, NASA Goddard Institute for Space Studies, USA.*